IOP Publishing Superconductor Science and Technology
Supercond. Sci. Technol. **29** (2016) 044006 (7pp) doi:10.1088/0953-2048/29/4/044006

Stability and normal zone propagation in YBCO CORC cables

M Majoros[1], M D Sumption[1], E W Collings[1] and D van der Laan[2]

[1] Center for Superconducting & Magnetic Materials (CSMM), The Ohio State University, Columbus, OH, USA
[2] Advanced Conductor Technologies and University of Colorado, Department of Physics, Boulder, CO, USA

E-mail: sumption.3@osu.edu

Received 30 October 2015, revised 19 January 2016
Accepted for publication 3 February 2016
Published 11 March 2016

Abstract

In this work, a two layer conductor on round core cable was tested for stability and normal zone propagation at 77 K in a liquid nitrogen bath. The cable was instrumented with voltage taps and wires on each strand over the cable's central portion (i.e. excluding the end connections of the cable with the outside world). A heater was placed in the central zone on the surface of the cable, which allowed pulses of various powers and durations to be generated. Shrinking (recovering) and expanding (not recovering) normal zones have been detected, as well as stationary zones which were in thermal equilibrium. Such stationary thermal equilibrium zones did not expand or contract, and hit a constant upper temperature while the heater current persisted; they are essentially a form of Stekly stability. Overall, the cable showed a high degree of stability. Notably, it was able to carry a current of $0.45I_{\mathrm{c\ cable}}$ with maximum temperature of 123 K for one minute without damage.

Keywords: YBCO, cables, stability, quench, normal zone, CORC, coated conductor

(Some figures may appear in colour only in the online journal)

Introduction

High field superconducting magnets require a large number of ampere-turns. To avoid large self-inductances in such magnets they must be wound using superconducting cables. Compared to other currently available high-temperature superconducting cables [1–10], conductor on round core (CORC) cables [11–14] (see figure 1) have a circular cross-section and the strands of which they are composed are helically twisted around the former. This makes them very suitable for the winding of superconducting magnets. Stability and normal zone propagation (NZP) is crucial in magnet applications. Indeed, NZP is a key parameter determining the magnet's quench protection scheme. In the present paper we measured NZP and more generally quench evolution in a 156 cm long, 2-layer CORC cable operating in a liquid nitrogen bath at 77 K. During these measurements we tested both cool-down and warm-up cycles, as well as allowable over-currents.

Samples

The YBCO tape used in the cable was 4 mm wide and had a nominal critical sheet current density of 25 A per 1 mm of tape width in self-field at 77 K. This results in cable nominal critical current of 600 A (77 K, self-field). The tape was stabilized by a 20 μm thick copper layer that was plated around the tape. The outside dimensions of the Cu-plated tape cross-section were 4.1 mm in width and 100 μm in thickness. Within the cable the tapes were wound helically with their superconducting layer on the inside, i.e. facing the former, to take advantage of their ability to sustain relatively large axial compressive strain without mechanical damage [11–14]. The cable used a flexible 5.5 mm diameter segment of stranded copper as the former; the former was insulated from the tapes. The two layers in the cable were wound with opposite chiralities (helicities). No interlayer insulation was used which allowed some level of current sharing between the tapes in the cable. The voltage wires were wound helically along the tapes

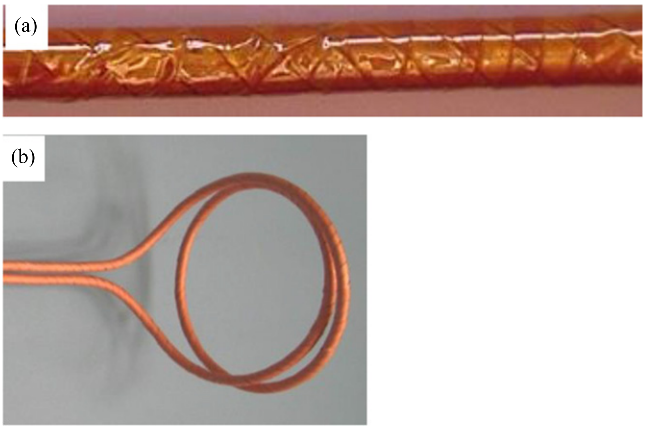

Figure 1. (a) Two layer CORC cable, 156 cm long, used in the experiments. (b) A detail view of a section of the cable.

and placed in the gaps in between them. The parameters of the CORC cable are summarized in table 1, and the instrumentation of the cable is shown in figure 2. Voltage taps and wires used in the measurements were positioned on each tape over the central portion of the cable (69 cm long, section *Vx*-2 in figure 2(b)). They covered only the superconducting portion of the cable, excluding the resistive joints on both ends of the cable. A heater (42 Ω, 5 mm × 5 mm) was placed on top of the cable, positioned in the middle of its length. The tapes were soldered onto the surface of the conical-shaped copper terminals, with their superconducting layer on the inside, using In–Bi–Sn solder (figure 2(b)).

Experimental

First we measured the room temperature resistances of each tape in the cable, as determined from the cable current. These results, shown in table 2, can be used to estimate the cable temperature during NZP experiments above the T_c (90 K) of the YBCO tapes. In case of a stationary NZ they can provide input parameters for equation (2). Using the copper cross-section of the tape and neglecting the contribution of the Hastelloy substrate and buffer layers to the conductivity, we obtain for the tape resistance at room temperature a value of 69.9 mΩ (per cable section 69 cm long, figure 2(b)). A parallel connection of six such tapes should have a resistance of 11.65 mΩ. From table 2 we see that only tapes in the outer layer of the cable (tape 4, 5, 6) show resistances close to 11.65 mΩ. Tapes from the inner layer of the cable (tape 1, 2, 3) show significantly lower resistances which might indicate a possible current sharing with the cable copper former. For evaluation of the temperature of the cable above T_c (=90 K) we used the calculated value of the cable room temperature resistance (11.65 mΩ) to calibrate the temperature resistance of the cable above 90 K. Temperatures obtained by this procedure are indicated in the figures (where applicable) throughout the paper.

The *I–V* curves of the tapes in the cable were measured using a sensitive Keithley nanovoltmeter in self magnetic field. NZPs were measured using a multi-channel high-speed data acquisition (DAQ) card controlled via LabView software. Heat was generated by applying a current pulse in the resistive heater. The heater, positioned on the outer surface of the cable (figure 2(a)), allowed pulses of various powers and durations to be generated at a cable current, during which we applied some percentage of the cable's self-field critical current. During and after the heat pulse NZP was measured by DAQ card.

Results

The self-field, DC *I–V* curves of the individual tapes versus cable current are shown in figure 3. Critical currents (determined at the electric field criterion of 1 μV cm^{-1}) obtained from them are summarized in table 3. The average cable critical current is $\langle I_c \rangle = 315$ A. The maximum I_c is 441.51 A (table 3) which is also the cable critical current. This represents 73.6% of the cable nominal critical current (600 A). This may be caused partially by the difference in tape self-field compared with the cable self-field or possibly some degradation in winding, handling, or previous measurement. It should be noted that both the *I–V* curves (figure 3) as well as the critical currents obtained from them (table 3) are determined from the overall cable current, since the currents in individual tapes could not be measured. These numbers reflect the current sharing between individual tapes in the cable, as well as current sharing which is completed within the current lugs of the cable (figure 2). The current sharing between tape 5 and 6 may be responsible for the quasi-linear portions of their *I–V* curves (between 100 A and 200 A) in figure 3. These quasi-linear parts appear prior to a sharp transition around 200 A. On the other hand a significant difference between the critical currents of tapes 2, 4 (all around 300 A) and the critical current of tape 1 and 3 (more than 400 A) and I_c of the tapes 5, 6 (around 200 A) (table 3 and figure 3) may be caused by the current re-distribution within the current lugs of the cable. This current redistribution may be caused by different contact resistances connected in series with the tapes within the cable current lugs [15] measured on the same cable prior to the experiments reported in the present paper. Approximate critical currents of the individual tapes can be estimated as follows. From figure 3 and table 3 we see that tape 5 and 6 have approximately the same critical currents (i.e. $I_{c5} \approx I_{c6}$). Also we may write $I_{c2} \approx I_{c4}$ and $I_{c1} \approx I_{c3}$. If we assume that at 200 A the current is homogeneously distributed among the tapes and the tapes 5 and 6 carry their critical currents, then we obtain $I_{c5} = I_{c6} = 33.33$ A. Similarly if we assume that at 300 A tapes 5 and 6 still carry their critical currents and the rest of the current is homogeneously distributed among the tapes 1, 2, 3 and 4, then we obtain $I_{c2} = I_{c4} = 58.33$ A. Applying the same procedure at 440 A we get $I_{c1} = I_{c3} = 103.33$ A. From this analysis we obtain the cable $I_c \approx 389.98$ A which is not too far away from the measured cable critical current of 441.51 A (table 3). It represents 88.3% of the measured cable critical current.

After completing *I–V* curve measurements we started with experiments on NZP and quench systematics. DC transport currents set to be some percentage of the cable

Table 1. Parameters of the CORC cable used in this study.

Cable	Former	Cable ID (mm)	No. layers	No. tapes/layer	Total No. tapes	L_p (mm)
CORC	Cu, stranded, insulated	5.5	2, not insulated	3, not insulated	6	32

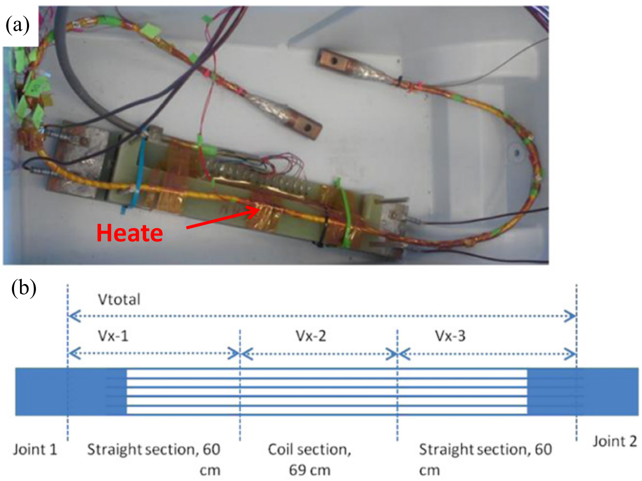

Figure 2. (a) Instrumentation of the cable (photo), (b) instrumentation of the cable—schematics.

Table 2. RT resistance of individual tapes.

Tape	Resistance (mΩ)
1	1.56
2	2.67
3	8.75
4	10.56
5	10.55
6	10.55

critical current $I_{c\ cable}$ were applied. During and after the heat pulse NZP was measured by a high speed DAQ card controlled via LabView software. At each DC current I (which was a fraction of the cable critical current) several different experiments were performed with heater pulse currents of different magnitude and duration applied and NZP detected. Combining the heater pulse current magnitude with its duration we were able to detect the onset of the NZP, as well as watch it either grow or shrink at different ratios of $I/I_{c\ cable}$. This is illustrated in figures 4–9.

As seen from figures 4 to 8, the differences between tapes seen in figure 3 do not appear at elevated temperatures. This is in accordance with [15] where it is shown experimentally and by modeling that the current distribution becomes homogeneous when the superconducting tapes transit into their normal state. Tape 1 shows a voltage in the middle of the spread of the data (figures 4–8) and tape 5 (figures 6–8) shows the lowest voltage.

Figures 4 and 5 represent two different regimes of NZs at $I_{cable} = 100$ A. Figure 4 shows a pulse energy high enough to initiate a normal zone, and once the power application is stopped, the zone shrinks—we are in a recovering zone.

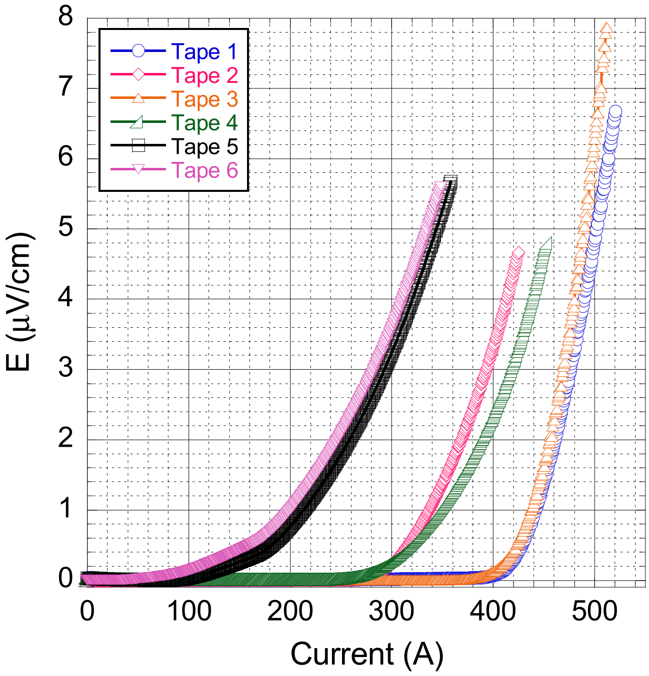

Figure 3. Self-field I–V curves of the cable tapes versus cable current. Linear portions of I–V curves of tape 5 and 6 (in a range between 100 A and 200 A) may be caused by current sharing among the tapes 5 and 6 within the cable.

Table 3. I_c for individual tapes (315 A average).

Tape	I_c (A)
1	441.51
2	337.35
3	441.51
4	349.35
5	213.34
6	199.90
Max.	441.51 $= I_{c\ cable}$

Figure 5, with a similar power deposition, but a much longer application time (and thus energy) creates a stationary normal zone. This stationary zone is different from a stagnant zone, in that its temperature does not continually increase. It is apparently in thermal equilibrium, such that the power generated by the I^2R in the cable (plus the smaller heater contribution) is exactly matched by the heat removal by the bath. A stagnant zone, on the other hand is spatially confined but has a large and continuing temperature increase, which will lead to burn out. The stationary zone as seen in figure 5 is relatively benign, and recovers once the power to the heater is switched off. The existence of such a stationary zone phenomenon is essentially a form of Stekly stability, where the heat generation in the conductor is balanced by the heat

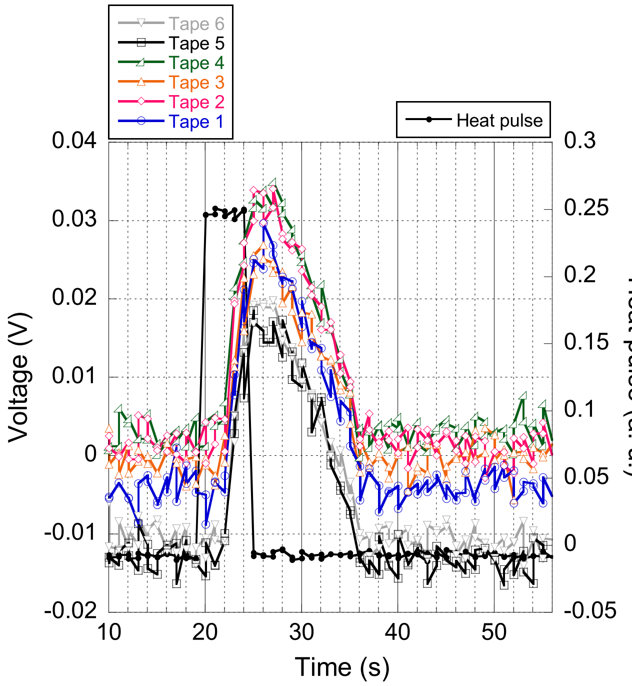

Figure 4. NZ with recovery (shrinking NZ): $I_{cable} = 100$ A, $I_{cable}/I_{c\ cable} = 0.226$, $I_{heater} = 1.00$ A/5 s, deposited energy = 210 J/25 mm^2.

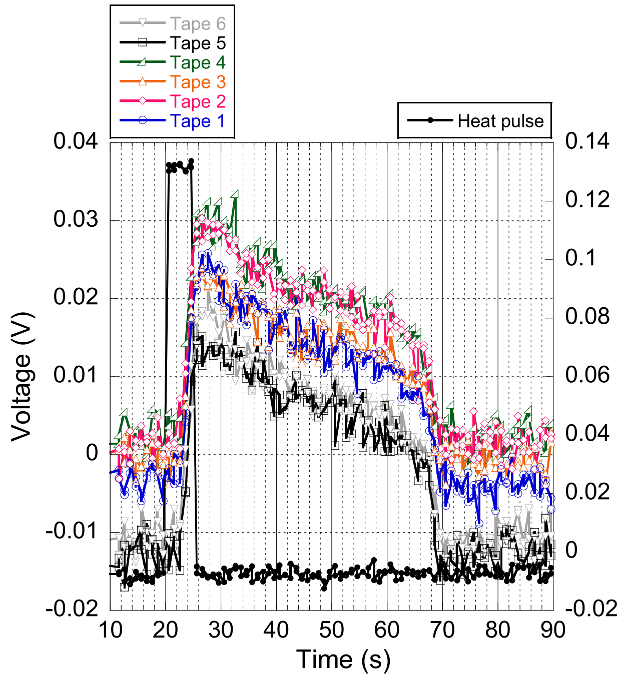

Figure 6. NZ with recovery (shrinking NZ): $I_{cable} = 150$ A, $I_{cable}/I_{c\ cable} = 0.34$, $I_{heater} = 0.55$ A/5 s, deposited energy = 63.5 J/25 mm^2.

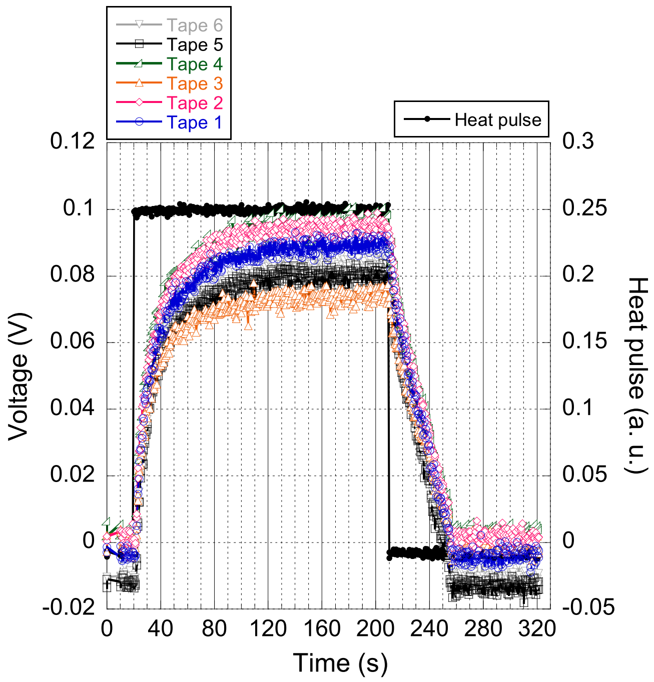

Figure 5. NZ with recovery (stationary NZ): $I_{cable} = 100$ A, $I_{cable}/I_{c\ cable} = 0.226$, $I_{heater} = 1.00$ A/200 s, deposited energy = 8400 J/25 mm^2.

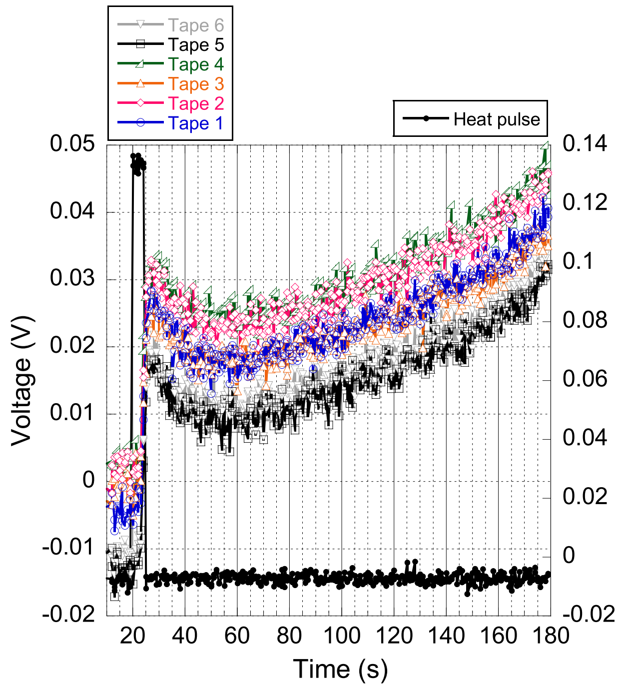

Figure 7. NZ with no recovery (expanding NZ): $I_{cable} = 150$ A, $I_{cable}/I_{c\ cable} = 0.34$, $I_{heater} = 0.56$ A/5 s, deposited energy = 65.9 J/25 mm^2.

removal to the cryogen [16]. Looking back to this treatment for LTSC wires, we know that the heat generation per unit length.

$$\dot{G} = \rho \frac{I^2}{A_{cu}} \text{ and } \dot{Q} = hP(T_m - T_b), \tag{1}$$

Where $\dot{G}$ is the power generation, $\dot{Q}$ is the heat removal, h is the coefficient of heat transfer at the cable to liquid nitrogen boundary, ρ is the stabilizer resistivity, P is the perimeter of the cable, T_m is the maximum temperature reached, A_{Cu} is the cross-section of the cable Cu stabilizer and T_b is the bath temperature. This can be easily solved to find the temperature

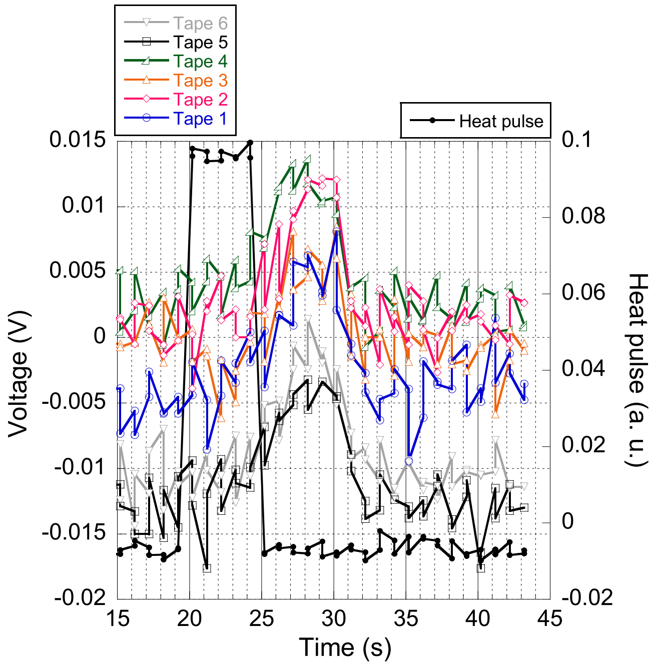

Figure 8. NZ with recovery (shrinking NZ): $I_{cable} = 200$ A, $I_{cable}/I_{c\ cable} = 0.453$, $I_{heater} = 0.412$ A/5 s, deposited energy = 35.6 J/25 mm^2.

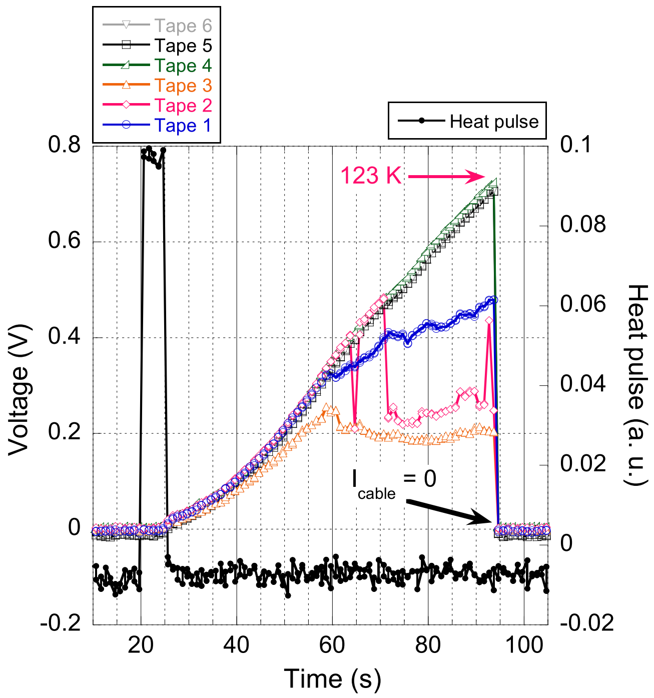

Figure 9. NZ with no recovery (expanding NZ): $I_{cable} = 200$ A, $I_{cable}/I_{c\ cable} = 0.453$, $I_{heater} = 0.414$ A/5 s, deposited energy = 36.0 J/25 mm^2.

that the stationary zone will reach

$$T_m = \rho \frac{I^2}{hPA_{cu}} + T_b. \tag{2}$$

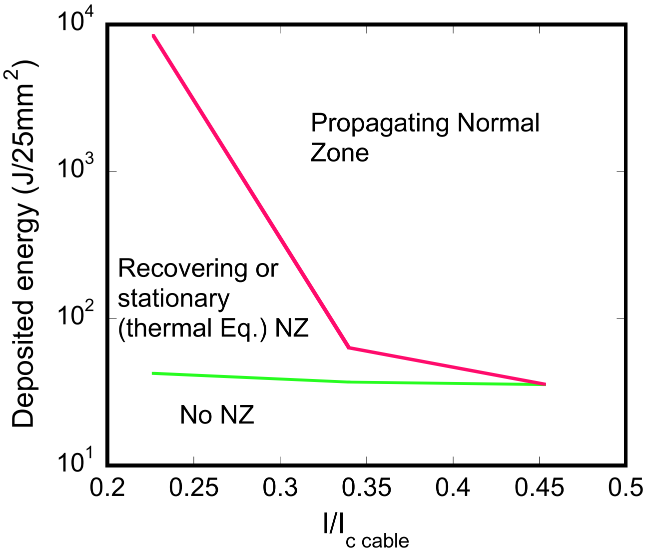

Figure 10. NZ phase diagram.

Taking an average voltage of 0.8 V from figure 5 and an area of 2-times the heater area, then using equation (2) and heat transfer coefficient given in [17] we get the temperature of the NZ close to 90 K.

Figure 6 shows an existence of recovering NZ at $I_{cable} = 150$ A, while figure 7 indicates onset of propagating NZ. Here we see that the criterion for stationary zones can no longer be met, and thus the heat generation must be greater than the potential cooling, even given the large temperature margin. Figure 8 represents an onset of NZ creation at $I_{cable} = 200$ A. Figure 9 demonstrates the cable's high degree of stability—the cable was able to carry the current of $0.45I_c$ with maximum temperature of 123 K for 1 min without damage. It is evident that some tapes (1, 2 and 3) tend to recover while tapes 4, 5 and 6 show a progressive heating. The fact that the tapes 4, 5, and 6 are positioned in outer layers suggest a possibility of additional cooling of tapes 1, 2 and 3 in the inner layer from inside by Cu former.

Minimum energies of shrinking and expanding NZ creation are summarized in table 4 and a phase diagram of NZ is shown in figure 10. It is seen that there exists a region with no NZ, and the region of a runaway NZ, as expected. In addition, in a narrow region we see a region labeled recovering or stationary normal zone formation. In that case, short energy pulses will lead to recovering zones. Longer pulses may lead to stationary zones, which can be described with the Stekly stability approach. These regimes, of course, are strongly dependent upon the fraction of the cable current to its critical current (figure 10).

Discussion

The homogeneous model for current distribution among the tapes gives a lower estimate of the temperature (figure 9). The maximum voltages in figures 4 and 6–8 are approximately

Table 4. Deposited energies for different NZ types.

$I_{cable}/I_{c\ cable}$	Max. energy—no NZ (J)	Min. energy—recovering or stationary NZ (J)	Max. energy, shrinking NZ (J)	Min. energy, expanding NZ (J)
0.226	40.7	42.5	>8400	
0.34	35.3	37.0	63.5	65.9
0.453	35.3	35.6	35.8	36.0

one order of magnitude lower than the voltages in figure 9. But all of them are orders of magnitude higher than $1\ \mu V\ cm^{-1}$ (the I_c criterion). We can assume that in figure 9 the whole cable length is in normal state. In figure 9, tapes 4, 5, 6 show the same voltage. These tapes are from the outer layer of the cable (in direct contact with LN_2). The inner layer tapes (1, 2, 3) show visibly lower voltages. This is in qualitative accordance with table 2, where the resistances were measured at room temperature and at a current of about 1 A, so no thermal inhomogeneities or overheatings were present. From table 2 we see that at 300 K and low currents (1 A) tapes 4, 5, 6 show significantly higher resistances than tapes 1, 2, 3. We ascribe this to possible some level of electrical contact with the cable Cu core. If we assume (in figure 9) that approximately 1/2 of the cable current is flowing through tapes 4, 5, and 6 then we obtain a resistance close to 300 K. From table 2 we have the measured resistances on a level of $10\ m\Omega$ at room temperature, so it can be assumed that they are higher than the resistances in the current lugs. The current lugs are more robust than the tapes so the heating effects in the current lugs should not be too high.

If the resistance of the normal zone at T_{max} is much higher than the cable end resistance, then even if there are variations in the individual contact resistances, the total circuit resistance of a given tape is controlled by the resistance of the normal region, and the tape currents will tend to be self-balancing. That is, the growth of a normal zone in one tape will tend to cause current redistribution in the cable which is effected (i.e., performed) at the cable current in and out junctions. Or, there is current sharing induced by a normal zone which is actually occurring in the cable junctions. This current sharing is kind of artificial, in that it will be a function of measured cable length. So, some strands of the cable may go normal, while others may be still superconducting. This rebalancing should affect the shape of the voltage versus time graph of a quench. It should be that a single strand going normal should have, (a) in the case of a weakly cooled (conduction, or gas) sample a curvature which is concave up, (b) in the case of a better cooled (LN_2) sample, the curvature, if J_e in the Cu is low enough, and the Stekly conditions can be made to apply, a concave downward curvature, and an eventual saturation, (c) in the case of good cooling and current sharing enabled either along the cable or at the cable ends, an even more concave downward shape, and a saturastion level of temperature which is somewhat lower than it would be for inhomogeneous current distribution within the cable.

Conclusion

Recovering as well as non-recovering NZs have been observed in a CORC cable under quench conditions operating in liquid nitrogen and self-field. In addition, for low $I/I_{c\ cable}$, the existence of stationary normal zones in the cable has been seen, which are essentially a form of Stekly stability phenomenon. Several examples of propagating and non-propagating zones were explored at higher $I/I_{c\ cable}$ fractions, and a stability diagram for the cable was generated. The CORC cable in this study showed a high degree of stability. It was able to carry a current of 45% of the cable critical current with maximum temperature of 123 K for one minute, without damage.

Acknowledgments

This work was supported by the US Department of Energy, Office of Science, Division of High Energy Physics, under Grant DE-SC0011721, DE-SC0007891 and DE-SC0014009.

References

[1] Takayasu M, Minervini J V and Bromberg L 2008 Superconductor cable *US Patent Application No.* PCT/US2009/047961

[2] Takayasu M, Chiesa L, Bromberg L and Minervini J V 2012 *Supercond. Sci. Technol.* **25** 014011

[3] Takayasu M, Mangiarotti F J, Chiesa L, Bromberg L and Minervini J V 2013 *IEEE Trans. Appl. Supercond.* **23** 4800104

[4] Takayasu M, Chiesa L and Minervini J V 2014 *IEEE Trans. Appl. Supercond.* **24** 6600105

[5] Goldacker W, Nast R, Kotzyba G, Schlachter S I, Frank A, Ringsdorf B, Schmidt C and Komarek P 2006 *J. Phys.: Conf. Ser.* **43** 901

[6] Long N J, Badcock R, Beck P, Mulholland M, Ross N, Staines M, Sun H, Hamilton J and Buckley R G 2008 *J. Phys.: Conf. Ser.* **97** 012280

[7] Lakshmi L S, Staines M P, Badcock R A, Long N J, Majoros M, Collings E W and Sumption M D 2010 *Supercond. Sci. Technol.* **23** 085009

[8] Terzieva S, Vojenciak M, Pardo E, Grilli F, Drechsler A, Kling A, Kudymov A, Gomory F and Goldacker W 2010 *Supercond. Sci. Technol.* **23** 014023

[9] Vojenciak M, Grilli F, Terzieva S, Goldacker W, Kovacova M and Kling A 2011 *Supercond. Sci. Technol.* **24** 095002

[10] Majoros M, Sumption M D, Collings E W and Long N J 2014 *IEEE Trans. Appl. Supercond.* **24** 6600505

[11] van der Laan D C 2009 *Supercond. Sci. Technol.* **22** 065013

[12] van der Laan D C, Lu X F and Goodrich L F 2011 *Supercond. Sci. Technol.* **24** 042001
[13] van der Laan D C, Goodrich L F and Haugan T J 2012 *Supercond. Sci. Technol.* **25** 014003
[14] van der Laan D C, Noyes P D, Miller G E, Weijers H W and Willering G P 2013 *Supercond. Sci. Technol.* **26** 045005
[15] Willering G, van der Laan D C, Noyes P, Weijers H, Miller G and Viouchkov Y 2015 *Supercond. Sci. Technol.* **28** 035001
[16] Stekly Z J J, Thome R and Strauss B 1969 *J. Appl. Phys.* **40** 2238
[17] Majoros M, Sumption M D, Collings E W and van der Laan D C 2014 *Supercond. Sci. Technol.* **27** 125008